Journal of Medicinal Chemistry

Article

pubs.acs.org/jmc

Guaifenesin Derivatives Promote Neurite Outgrowth and Protect Diabetic Mice from Neuropathy

Mallinath B. Hadimani,[§] Meena K. Purohit,[†,‡] Chandrashaker Vanampally,[§] Randy Van der Ploeg,[⊥] Victor Arballo,[∥] Dwane Morrow,[⊥] Katie E. Frizzi,[∥] Nigel A. Calcutt,[∥] Paul Fernyhough,[⊥] and Lakshmi P. Kotra*[,†,§,#,∞]

[†]Center for Molecular Design and Preformulations, Toronto General Research Institute, University Health Network, Toronto, Ontario M5G 2C4, Canada

[‡]Department of Pharmacy, Birla Institute of Technology and Science, Pilani, Rajasthan, India

[§]Department of Chemistry and Biochemistry, The University of North Carolina at Greensboro, Greensboro, North Carolina 27412, United States

[∥]Department of Pathology, University of California at San Diego, San Diego, California 92093, United States

[⊥]Department of Pharmacology and Therapeutics and Division of Neurodegenerative Disorders, St. Boniface Research Center, University of Manitoba, Winnipeg, Manitoba R2H 2A6, Canada

[#]McLaughlin Center for Molecular Medicine, University of Toronto, Toronto, Ontario, Canada

[∞]Department of Pharmaceutical Sciences, Leslie Dan Faculty of Pharmacy, University of Toronto, Toronto, Ontario M5S 3M2, Canada

Supporting Information

ABSTRACT: In diabetic patients, an early index of peripheral neuropathy is the slowing of conduction velocity in large myelinated neurons and a lack of understanding of the basic pathogenic mechanisms hindered therapeutics development. Racemic (*R*/*S*)-guaifenesin (**1**) was identified as a potent enhancer of neurite outgrowth using an in vitro screen. Its *R*-enantiomer (*R*)-**1** carried the most biological activity, whereas the *S*-enantiomer (*S*)-**1** was inactive. Focused structural variations to (*R*/*S*)-**1** was conducted to identify potentially essential groups for the neurite outgrowth activity. In vivo therapeutic studies indicated that both (*R*/*S*)-**1** and (*R*)-**1** partially prevented motor nerve conduction velocity slowing in a mouse model of type 1 diabetes. In vitro microsomal assays suggested that compounds (*R*)-**1** and (*S*)-**1** are not metabolized rapidly, and PAMPA assay indicated moderate permeability through the membrane. Findings revealed here could lead to the development of novel drugs for diabetic neuropathy.

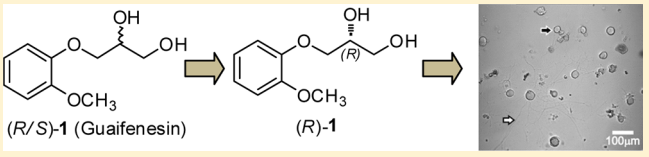

INTRODUCTION

According to the World Health Organization, an estimated 350 million people are expected to suffer from diabetes by 2030, doubling the current numbers.[1] In the U.S., 8.3% of the population is afflicted with diabetes. In 2007, it was estimated that this epidemic cost about $174 billion[2] and the costs are rising. Complications of chronic diabetes usually appear 5−10 years after the onset of the disease[3] and significantly reduce the quality of life. Neuropathy is the most common of the complications of long-term diabetes with an incidence greater than 50%[4] and can lead to incapacitating pain, sensory loss, foot ulceration, gangrene, and lower limb amputation.[5]

In diabetic patients, slowing of conduction velocity in large myelinated sensory and motor neurons is an early and quantifiable index of peripheral neuropathy. Conduction slowing is predictive of progression to degenerative neuropathy in diabetic patients[6] and is widely used to diagnose the condition[7] and assess efficacy of therapeutics in clinical trials.[8] The pathogenic mechanisms that cause nerve conduction slowing and other aspects of diabetic neuropathy are not established. Indeed, while there is good evidence that instigating tight glycemic control can slow onset and progression of diabetic neuropathy (DCCT study), the relative contribution of hyperglycemia and impaired insulin signaling as primary pathogenic mechanisms remains controversial.[9] This lack of understanding of the basic pathogenic mechanisms underlying diabetic neuropathy has hindered development of targeted therapeutic strategies. To date, there is no FDA-approved therapy that prevents, halts progression of, or reverses degenerative neuropathy, while drugs that alleviate pain associated with diabetic neuropathy are palliative rather than addressing the underlying pathogenesis.

One strategic approach to discovering potential therapeutics for diabetic neuropathy involves identifying molecules that promote survival, sprouting, and/or regeneration of adult

Received: March 18, 2013

   dx.doi.org/10.1021/jm400401y | *J. Med. Chem.* XXXX, XXX, XXX−XXX

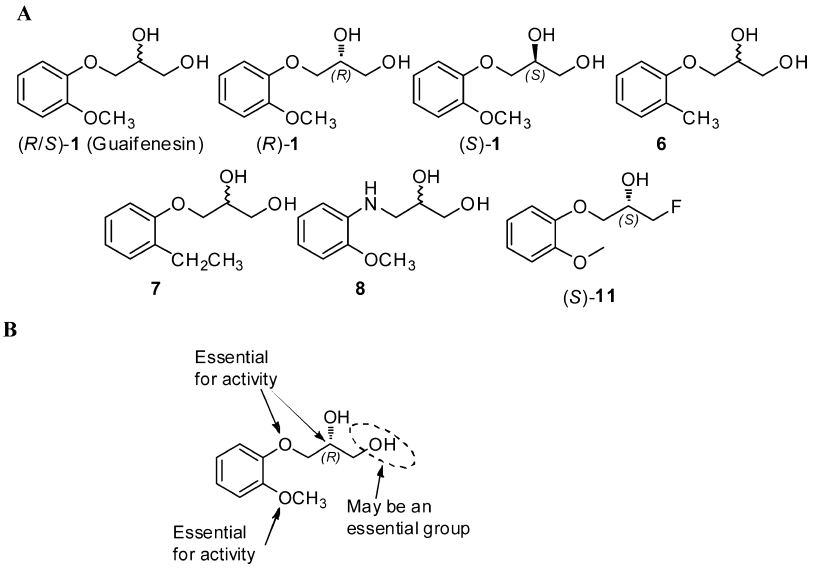

Figure 1. (A) Structure of guaifenesin ((*R*/*S*)-**1**), its enantiomers (*R*)-**1** and (*S*)-**1**, and its derivatives **7**, **8**, and (*S*)-**11**. (B) Suggested pharmacophore model derived from the structure−activity relationship targeting diabetic neuropathy.

peripheral neurons as an index of neurotrophic and neuroprotective properties. The adult sensory neuron culture system allows a direct and rapid in vitro screening approach for the identification of such small molecules.[10] Compounds such as polycyclic aza-amide neuroimmunophilin, arylbenzylimidazole AT_2 agonists, short chain ceramide analogues, alkylaminooxysterols dendrogenin B, and other agents have been reported to induce neurite outgrowth.[11−18] We recently screened a library of 600 compounds for their ability to enhance axonal regeneration in adult rat sensory neurons by at least 2-fold in vitro.[19] This led to the identification of guaifenesin ((*R*/*S*)-**1**) as a potent enhancer of neurite outgrowth. Guaifenesin is a common ingredient of various cough medications, where it is included as an expectorant. Here, we report our investigations on guaifenesin, its enantiomers, and related phenoxy propane diol derivatives on neurite outgrowth in vitro and then assessed efficacy of selected compounds in a mouse model of diabetes-induced nerve conduction slowing to determine their potential as agents for the treatment of diabetic neuropathy.

RESULTS AND DISCUSSION

To assess the response of the neuronal outgrowth to changes in the functional groups on (*R*/*S*)-**1**, we modified the structure of (*R*/*S*)-**1** on its propyl side chain and the ortho substitution on the phenyl moiety (Figure 1A). This allowed us to explore key chemical groups on guaifenesin that may be responsible for this biological response and to potentially establish a limited structure−activity relationship. Thus, a small set of compounds **6**−**10** were synthesized. Compounds **6** and **7** carry a methyl and an ethyl substitution at the ortho position on the phenyl moiety. Compound **8** carries a −NH- group instead of an ether moiety linking the propyl side chain, and compounds (*R*)-**1** and (*S*)-**1** are the *R* and *S* enantiomers, respectively, of guaifenesin. Further modification of the *R* enantiomer, (*R*)-**1** of guaifenesin (*R*/*S*)-**1** afforded compound **13** where a fluorine moiety is substituted in place of a hydroxyl moiety at the primary alcohol position on the propyl side chain of (*R*)-**1**.

Compounds (*R*/*S*)-**1** and **6**−**8** were synthesized using a similar strategy, where appropriately ortho substituted phenol or aniline was reacted with racemic dihydroxychloropropane at high temperature under basic conditions using microwave irradiation for 15 min (Scheme 1). Final compounds were

Scheme 1. Preparation of Compounds (*R*/*S*)-1 and (*R*/*S*)-6 through (*R*/*S*)-8[a]

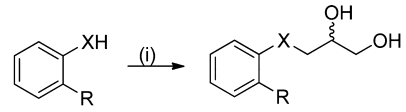

2 R = OCH_3, X = O (*R*/*S*)-**1** R = OCH_3, X = O
3 R = CH_3, X = O (*R*/*S*)-**6** R = CH_3, X = O
4 R = C_2H_5, X = O (*R*/*S*)-**7** R = C_2H_5, X = O
5 R = OCH_3, X = NH (*R*/*S*)-**8** R = OCH_3, X = NH

[a]Reagents and conditions: (i) NaOH, anhyd DMF, microwave at 210 °C, 15 min, (±)-chloropropane-2,3-diol.

obtained in good to excellent yields. *R*- and *S*-enantiomers of **1**, compounds (*R*)-**1** and (*S*)-**1**, respectively, were synthesized by reacting *o*-methoxyphenol with either (*R*)- or (*S*)-chloropropanediol to yield the final products (Scheme 2). For the

Scheme 2. Preparation of Enantiomers of (*R*/*S*)-1[a]

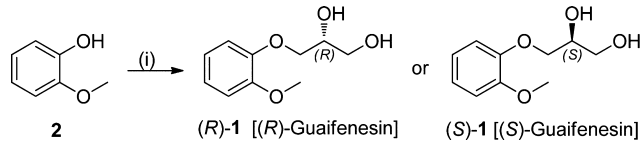

[a]Reagents and conditions: (i) NaOH, anhydrous DMF, microwave at 210 °C, 15 min, (*R*)-chloropropane-2,3-diol, 64% [for (*R*)-**1**], or (*S*)-chloropropane-2,3-diol, 64% [for (*S*)-**1**].

introduction of the fluorine moiety to yield **13**, (*R*)-epichlorohydrin was reacted with compound **2** under basic conditions to yield the epoxide **12** (Scheme 3). Epoxide moiety was opened by introducing the fluoride using TBAF to yield enantiomerically pure **13**.

In Vitro Evaluation of Axon Regeneration. The effect of each compound on enhancing the neurite outgrowth was assessed in adult rat dorsal root ganglia (DRG) sensory

dx.doi.org/10.1021/jm400401y | J. Med. Chem. XXXX, XXX, XXX−XXX

Scheme 3. Preparation of Fluorinated Derivative of (*R*)-1[a]

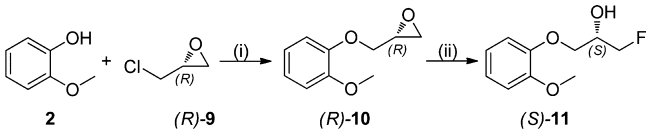

[a]Reagents and conditions: (i) NaOH, K_2CO_3, tetra-*n*-butylammonium bromide, microwave, 110 °C, 5 min (for (*R*)-**10**); (ii) 1 M TBAF in THF, toluene, 80 °C, 3 h, (for (*S*)-**11**).

neurons using the established procedure in our laboratories.[20,31,32] Compound (*R*/*S*)-**1**, typically used in racemate form as an expectorant, exhibited elevated neurite outgrowth at higher than 10 nM in vitro (Figure 2A). Neuronal cultures clearly showed the sprouting of the neurites after treatment with compound (*R*/*S*)-**1** at 1 μM (Figure 2F). Substitution of the methoxy group in (*R*/*S*)-**1** with the methyl group as seen in **6** compromised the activity by at least 2 orders of magnitude (Figure 2A, compound (*R*/*S*)-**1** vs **6**). An ethyl substitution in place of methoxy (Figure 2A and Figure 2B, compound (*R*/*S*)-**1** vs **7**) completely abrogated the neuronal outgrowth activity.

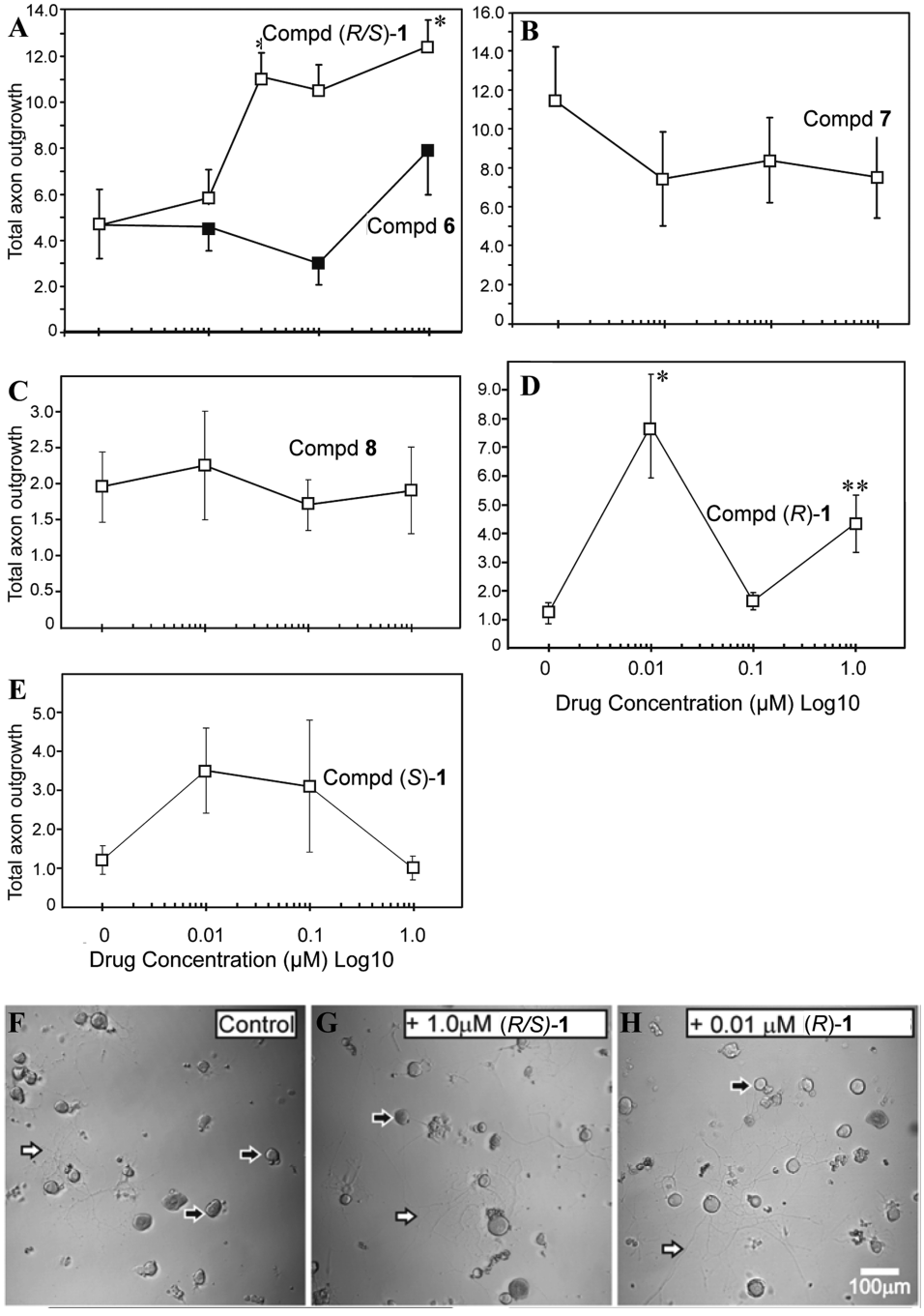

Figure 2. (A–E) Dose–response curves for neurite outgrowth of cultured DRG sensory neurons for compounds (*R*/*S*)-**1**, **7**, **8**, (*R*)-**1**, and (*S*)-**1** and (F–H) enhanced microscope images for the control cells and those treated with (*R*/*S*)-**1** and (*R*)-**1**. All data were adjusted to number of cells (presented as number of intersects per cell) and shown as total neurite outgrowth. Values are the mean ± SEM (n = 6 replicate cultures): (*) P < 0.05 vs control; (**) P < 0.02 vs control and 0.1 μM (one-way ANOVA with Tukey's post hoc test).

dx.doi.org/10.1021/jm400401y | *J. Med. Chem.* XXXX, XXX, XXX–XXX

Thus, the methoxy moiety at the ortho position of (*R*/*S*)-**1** may be an essential group for the biological activity, although one cannot rule out the possibility that an ether link is the required structural feature, and the alkyl group, i.e., methyl moiety on the ether, could be altered. A substitution of the ethereal oxygen of the propyl side chain with an amino moiety gave compound **8**. At physiological pH, including the pH used for the in vitro assays, this molecule would be protonated because of the presence secondary amine. In the in vitro assay, compound **8** was inactive at up to 1 μM, which indicated that the substitution of the ether moiety with -NH- may not yield a productive structural change for targeting the biological activity. Compound **13**, the *R*-enantiomer with a fluoro substitution, also did not show any neurite outgrowth activity.

Since compound (*R*/*S*)-**1** is a racemate, we decided to investigate the role of the stereocenter in eliciting the neurite outgrowth to determine whether the target receptor is sensitive to the chirality of the ligands. Thus, enantiomerically pure *R*- and *S*-enantiomers of (*R*/*S*)-**1** were evaluated in vitro in DRG cell cultures for neurite outgrowth effects. Compounds (*R*)-**1** and (*S*)-**1** showed interesting effects in vitro: the *R*-enantiomer (*R*)-**1** exhibited very high efficacy at 0.01 μM, which is quite potent and unlike any other compound known to date affecting neurite outgrowth in adult sensory neurons. Compound (*S*)-**1**, the *S*-enantiomer of guaifenesin, was found to be less efficacious in vitro compared to the racemate and the corresponding *R*-enantiomer (*R*)-**1** (Figure 2D vs Figure 2E).

Overall, the above small set of compounds (**1** and **6**−**8** and **13**) support the idea that the 1,2-diol side chain with ether linker and a methoxy group on the phenyl ring are essential for the activity (Figure 1B). The general trend observed from the dose−response curves indicates that there is at least a 2-fold difference in the neurite-inducing activities of *R*- and *S*-enantiomers, favoring the *R*-enantiomer (Figure 1B). Fibers associated with the neurite outgrowth are clearly visible when DRG neurons were treated with (*R*)-**1** at 10 nM (Figure 2H).

In Vivo Studies. On the basis of the in vitro findings, we selected the racemate **1** and its *R*-enantiomer (*R*)-**1** to evaluate their potential as therapeutic agents against peripheral neuropathy induced by insulin-deficient diabetes. We used the streptozotocin (STZ)-induced mouse model of diabetic neuropathy, since these insulin-depleted animals develop motor neuron conduction velocity (MNCV) slowing within weeks of onset of type 1 diabetes[21] and MNCV slowing is widely used to diagnose and predict progression of neuropathy in diabetic patients.[6,22] Compound (*R*/*S*)-**1** attenuated onset of MNCV slowing in STZ-diabetic mice at doses of 10 and 100 mg kg^{-1} day^{-1} with no indication of dose-related efficacy. A similar partial effect was noted with the *R*-enantiomer (*R*)-**1** at the doses 1 and 10 mg kg^{-1} day^{-1}. Normal mice treated with (*R*/*S*)-**1** (10 or 100 mg kg^{-1} day^{-1} po 6 days per week for 4 weeks) displayed no unusual behaviors and exhibited body weight (27.1 ± 0.5 g) and MNCV (35.1 ± 1.0 m/s) values that were similar to those for vehicle-treated mice (26.7 ± 0.4 g and 35.6 ± 1.1 m/s, respectively). This established that the administration of (*R*/*S*)-**1** did not cause any unusual effects in mice. Four weeks after STZ injection mice displayed significant hyperglycemia ($p < 0.05$), reduced body weight, and MNCV slowing compared to control mice (Figure 3), indicative of the presence of diabetes and diabetic neuropathy. Treatment of STZ-diabetic mice with (*R*/*S*)-**1** (10 or 100 mg kg^{-1} day^{-1}) did not alter systemic diabetes, as indicated by absence of effect on weight loss or hyperglycemia (Figure 3A and Figure 3B), but partially prevented MNCV slowing at both doses (Figure 3C).

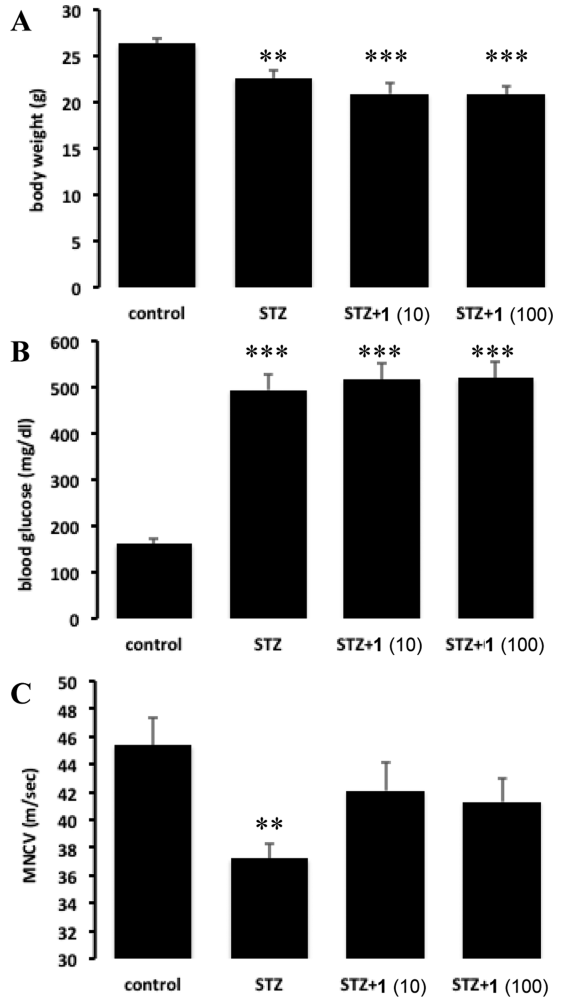

Figure 3. Physiological parameters: (A) body weight, (B) blood glucose, and (C) MNCV in control mice, STZ-diabetic mice, and STZ-diabetic mice treated with compound (*R*/*S*)-**1** (10 or 100 mg kg^{-1} day^{-1} po for 4 weeks). Data are the group mean ± SEM of N = (10−12)/group with statistical comparisons by one-way ANOVA followed by Dunnett's post hoc test: (**) $p < 0.01$ and (***) $p < 0.001$ vs control.

A separate experiment was initiated to evaluate the effects of the *R*-enantiomer (*R*)-**1**, since it was superior to the corresponding *S*-enantiomer in vitro. STZ-injected mice again displayed significant hyperglycemia ($p < 0.05$), reduced body weight, and MNCV slowing compared to control mice after 4 weeks of diabetes (Figure 4). Treatment of STZ-diabetic mice with (*R*)-**1** (either at 1 or 10 mg kg^{-1} day^{-1} dose) had no effect on weight loss or hyperglycemia, indicating continued systemic diabetes (Figure 4A and Figure 4B). Treatment with (*R*)-**1** prevented MNCV slowing at 1 and 10 mg kg^{-1} day^{-1} (Figure 4C). The improvement in MNCV was similar to that observed with the racemate (or racemic mixture) (*R*/*S*)-**1**. This is notable because the dose for (*R*)-**1** was 10-fold less compared to (*R*/*S*)-**1**, and the effect in vivo was observable even at 1 mg kg^{-1} day^{-1} dose (po).

With these encouraging results, we undertook pilot experiments to understand the bioavailability for these compounds (Table 1). Interestingly, the peak plasma concentrations (C_{max}) in control and diabetic mice for compound (*R*)-**1** were 12- and

dx.doi.org/10.1021/jm400401y | J. Med. Chem. XXXX, XXX, XXX−XXX

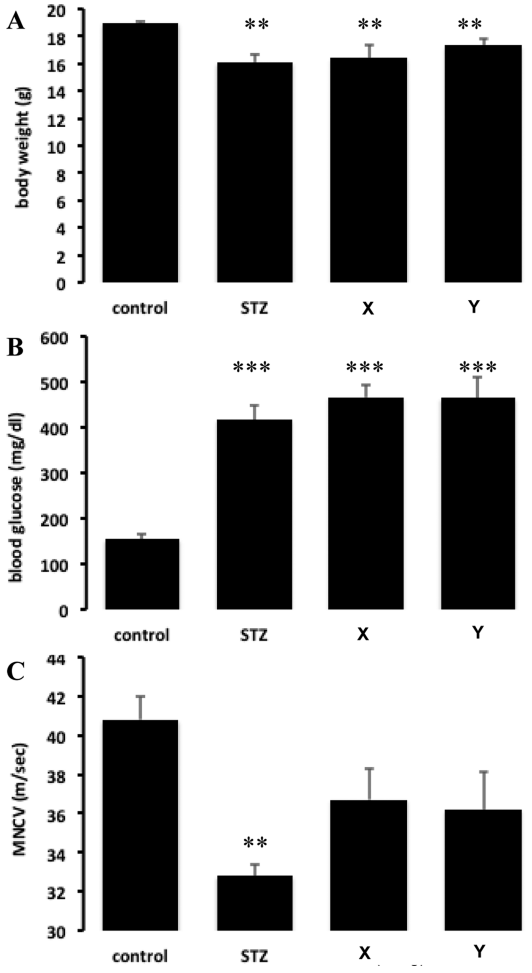

Figure 4. Physiological parameters: (A) body weight, (B) blood glucose, and (C) MNCV in control mice, STZ-diabetic mice, and STZ-diabetic mice treated with compound (*R*)-**1** with a dose of either 1 (X) or 10 (Y) mg kg^{-1} day^{-1} po for 4 weeks. Data are the group mean ± SEM of N = (10−12)/group with statistical comparisons by one-way ANOVA followed by Dunnett's post hoc test: (**) $p < 0.01$ and (***) $p < 0.001$ vs control.

Table 1. Pharmacokinetic Parameters for (*R*/*S*)-1 and Its *R*-Enantiomer (*R*)-1 in Control and STZ-Diabetic Mice

	(*R*/*S*)-**1**		(*R*)-**1**	
parameter	control	STZ-diabetic mice	control	STZ-diabetic mice
dose (mg/kg po)	10	10	10	10
T_{max} (min)	4.98	4.98	10.02	10.02
C_{max} (nM)	5283	5267	440	741
AUC_{0-t} (h·nM)	2725	1911	737	746

7-fold lower than those for the racemate (*R*/*S*)-**1**, respectively, when these compounds were administered orally (10 mg dose). Similarly $AUC_{0-\infty}$ was also lower for compound (*R*)-**1** in mice when compared to that of racemate (*R*/*S*)-**1**. However, the efficacy due to (*R*)-**1** was almost equal even at 1 mg kg^{-1} day^{-1} dose.

Overall, neither compound altered the severity of the diabetes in mice, indicating an effect on the manifestation of neuropathy rather than on the disease itself. Both compounds ameliorated MNCV slowing without completely protecting nerve function. Whether complete efficacy can be achieved at higher doses remains to be determined, as does the lower limit of efficacy. Nerve conduction slowing in short-term STZ-diabetic rodents is attributed to metabolic and vascular dysfunction conditions that arise secondary to hyperglycemia. Agents, such as aldose reductase inhibitors, that block glucose metabolism through the polyol pathway and restore nerve blood flow are effective against MNCV slowing in STZ-diabetic rodents[23−25] and provide modest protection of NCV in diabetic patients.[8,26] Although the mechanism of action for guaifenesin remains to be determined, derivatives of this compound have demonstrated effects on muscle electrophysiology and relaxation[27,28] that suggest potential for modulation of vascular function. Moreover, as the therapeutic potential of racemate (*R*/*S*)-**1** and its *R*-enantiomer (*R*)-**1** was identified using a neurite outgrowth assay in adult sensory neurons in vitro, direct actions on neurons should also be considered and future studies may assess in vivo efficacy against specific indices of sensory fiber neuropathy in diabetic mice such as depletion of epidermal sensory C fibers and loss of paw thermal sensation.[29]

In Vitro Microsomal and Permeability Assays. PAMPA assays using compounds (*R*)-**1** and (*S*)-**1** were conducted to assess their membrane permeability potential. Both compounds exhibited moderate permeability through the artificial membrane, with 63 ± 5 and 82 ± 5 nm/s for compounds (*R*)-**1** and (*S*)-**1**, respectively (Table 2). Control with propranolol exhibited 164 ± 12 nm/s permeability. Thus, both compounds are expected to cross the membrane almost equally and chirality should not have played any role in their permeability. Mass retention for both compounds was less, with 15.0 ± 4.5% and 5.5 ± 2.7% for compounds (*R*)-**1** and (*S*)-**1**, respectively.

Table 2. PAMPA Permeability and % Remaining after Liver Microsomes Exposure of Compounds (*R*)-1 and (*S*)-1, at 25 °C

		% remaining after liver microsomal exposure	
compd	permeability (nm/s)	mouse	human
control (propranolol)	164 ± 11.6	12.8 ± 0.8	45.4 ± 5.5
(*R*)-**1**	63 ± 4.9	92.4 ± 3.3	97.4 ± 3.9
(*S*)-**1**	82 ± 4.7	92.9 ± 3.9	94.8 ± 10.8

Human and mouse liver microsomal studies were conducted to understand the metabolic stabilities of compounds (*R*)-**1** and (*S*)-**1**. Both compounds exhibited relatively high stability after incubation for an hour in either mouse or human microsomes, being in the range of 92−98% of the original compound unaltered, so that only 2−8% was metabolized (Table 2). Propranolol control was metabolized relatively quickly, with approximately 50% metabolized in human microsomes and up to 86% metabolized in the mouse microsomes. These studies indicate that compounds (*R*)-**1** and (*S*)-**1** exhibit comparable, moderate levels of membrane permeability and high microsomal metabolic stability. The differences in the in vitro and in vivo efficacy for compounds (*R*)-**1** and (*S*)-**1** appear to be unrelated to their metabolism or membrane permeability properties and are more likely to be related to their chiral center (*R*)- vs (*S*)-guaifenesin.

In summary, we demonstrated neurite outgrowth activity for (*R*/*S*)-**1** and that most of the biological activity resided in its *R*-enantiomer. Derivatives of (*R*/*S*)-**1** clearly indicated that functional group modifications must be considered carefully in order to retain the neurite outgrowth activity, and a

dx.doi.org/10.1021/jm400401y | J. Med. Chem. XXXX, XXX, XXX−XXX

preliminary pharmacophore model is proposed based on the structure−activity relationships. Molecules with in vitro activity showed promising in vivo efficacy in a mouse model of diabetic neuropathy. Our findings support the development of a novel class of drugs to treat diabetic neuropathy.

EXPERIMENTAL PROCEDURES

Synthesis. General. All chemicals including reagents with stereocenters including (*R*)-(−)-α-monoclhorhydrine, (*S*)-(−)-α-monochlorohydrine, and (*R*)-epichlorohydrin were purchased from commercial suppliers and were used without further purification. DMF and triethylamine were dried over 4 Å molecular sieves. Microwave reactions were carried out in a Biotage Initiator microwave equipped with a robotic arm for four consecutive reactions. Reactions were monitored by thin layer chromatography (TLC) performed on precoated silica gel aluminum sheets (F_{254}, 60 Å, Merck). Column chromatography was performed using silica gel (230−400 Å mesh, EMD Chemicals). The ^{13}C and ^{1}H NMR spectra were recorded on a Joel (JEOL) spectrometer (500 MHz for ^{1}H, 125 MHz for ^{13}C) or a Bruker spectrometer (400 MHz for ^{1}H, 100 MHz for ^{13}C). The chemical shifts for ^{1}H NMR spectra are reported in ppm (δ) relative to tetramethylsilane. Mass spectra (ESI) were recorded on a Waters UPLC/MS instrument with a Waters 3100 mass detector. Specific rotations of synthesized enantiomers were obtained using Interscience AA-55 polarimeter in methanol at 23 °C. Purity of the synthesized compounds was determined by a Waters HPLC system (Delta 600) and/or LC−MS system (Waters 2545 binary gradient module) equipped with a PDA. The purity of compound (*R*/*S*)-**1** was found to be 97.03% and that of compound (*S*)-**11** was 90.07% by HPLC, and the purity of all other compounds reported was positively established by elemental analyses criteria. Mass spectra (ESI) were recorded on a Waters MS system equipped with a Waters 3100 mass detector.

General Procedures for the Synthesis of Compounds (*R*/*S*)-1 and 6−8. Appropriate ortho substituted phenol or aniline (1.0 equiv) in the presence of sodium hydroxide (0.9−2.5 equiv) was reacted with 1,2-dihydoxy-3-chloropropane (0.9−2.5 equiv) in DMF (2 mL) in a Biotage Initiator microwave. The reaction mixture was irradiated at 210 °C for 15 min to obtain the phenol derivatives (*R*/*S*)-**1**, **6**, **7** and at 150 °C for 5 min to obtain the aniline derivative **8**. The reaction mixture was then diluted with EtOAc (10 mL) and washed with H_2O (10 mL). The organic phase was separated, and the aqueous phase was extracted with EtOAc (3 × 50 mL). The combined organic layers were washed with H_2O (2 × 50 mL) followed by brine and dried (Na_2SO_4). The solvents were removed under reduced pressure, and the resulting crude was purified by silica gel flash chromatography using a gradient of 1−5% MeOH in $CHCl_3$.

(*R*/*S*)-3-(2-Methoxyphenoxy)-1,2-propanediol ((*R*/*S*)-1)). The product was obtained as a white solid (149 mg, 75%). Mp 79−80 °C. ^{1}H NMR ($CDCl_3$) δ 2.60 (t, 1H), 3.39 (d, 1H), 3.75−3.84 (m, 2H), 3.86 (s, 3H), 4.04−4.12 (m, 2H), 4.13−4.20 (m, 1H), 6.88−6.95 (m, 3H), 6.96−7.01 (m, 1H). ^{13}C NMR ($CDCl_3$) δ 55.9, 64.0, 70.1, 72.5, 111.9, 115.0, 121.2, 122.4, 148.1, 149.8. ESI-MS (M + Na^+) calculated, 221.19; found, 221.0.

(*R*/*S*)-3-(2-Methylphenoxy)-1,2-propanediol (6). Product was obtained as a white solid (171 mg, 94%). Mp 68 °C. ^{1}H NMR ($CDCl_3$) δ 2.15 (t, 1H), 2.23 (s, 3H), 2.66 (d, 1H), 3.76−3.82 (m, 1H), 3.84−3.91 (m, 1H), 4.06 (d, 2H), 4.11−4.17 (m, 1H), 6.83 (d, 1H), 6.89 (t, 1H), 7.16 (t, 2H). ESI-MS (*m*/*z*) calculated, 182.22; found, 182.10.

(*R*/*S*)-3-(2-Ethylphenoxy)-1,2-propanediol (7). Product was obtained as a white solid (175 mg, 89%). Mp 53 °C. ^{1}H NMR ($CDCl_3$) δ 1.20 (t, 3H), 2.08−2.18 (br, 1H), 2.64 (q, 2H), 3.76−3.83 (m, 1H), 3.85−3.91 (m, 1H), 4.06 (d, 2H), 4.11−4.18 (m, 1H), 6.84 (d, 1H), 6.91 (t, 1H), 7.14−7.21 (m, 2H). ESI-MS (*m*/*z*) calculated, 196.24; found, 196.10.

(*R*/*S*)-3-(2-Methoxyphenylamino)-1,2-propanediol (8). Product was obtained as a light brown solid (315 mg, 26%). ^{1}H NMR ($CDCl_3$) δ 3.24 (dd, 1H), 3.30 (dd, 1H), 3.66 (dd, 1H), 3.80 (dd, 1H), 3.896 (s, 3H), 3.98−4.02 (m, 1H), 6.67 (dd, 1H), 6.70−6.74 (m, 1H), 6.79 (dd, 1H), 6.86−6.89 (m, 1H). ESI-MS (M + Na^+) calculated, 220.30; found, 220.10.

(2*R*)-3-(2-Methoxyphenoxy)propane-1,2-diol ((*R*)-1). A suspension of NaOH (298 mg, 7.45 mmol) in anhydrous DMF (2 mL) was mixed with guaiacol (616 mg, 4.96 mmol) and (*R*)-(−)-α-monochlorohydrine (822 mg, 7.44 mmol) in a microwave vessel. The reaction vessel was placed in the microwave and was irradiated at 210 °C for 15 min. The reaction mixture was then diluted with EtOAc (30 mL), washed with H_2O (15 mL), brine (15 mL), and dried (Na_2SO_4). Evaporation of the solvent and purification of the crude by silica gel column chromatography (6% MeOH in CH_2Cl_2) yielded compound (*R*)-**1** (630 mg, 64%) as a white powder which was then recrystallized from EtOAc. ^{1}H NMR ($CDCl_3$) δ 3.78−3.79 (m, 2H), 3.81 (s, 3H), 4.04−4.06 (m, 1H), 4.13 (d, 2H), 6.90−6.91 (m, 4H). ^{13}C NMR ($CDCl_3$) δ 56.1, 64.2, 70.3, 72.6, 112.2, 115.2, 121.4, 122.6, 148.3, 150.0. ESI-MS (M + Na^+) calculated, 221.32; found, 221.0. $[\alpha]_D^{23.6}$ −7.14° (*c* 1.12, MeOH).

(2*S*)-3-(2-Methoxyphenoxy) propane-1,2-diol ((*S*)-1). Compound (*S*)-**1** was synthesized using the same reaction conditions as for compound (*R*)-**1** but in presence of (*S*)-(+)-α-monochlorohydrine, and the product was isolated as a white solid (64%). ^{1}H NMR ($CDCl_3$) δ 3.78−3.79 (m, 2H), 3.81 (s, 3H), 4.04−4.06 (m, 1H), 4.13 (d, 2H), 6.90−6.91 (m, 4H). ESI-MS (M + Na^+) calculated, 221.32; found, 221.0. $[\alpha]_D^{23.6}$ +7.5° (*c* 1.2, MeOH).

(*R*)-2-((2-Methoxyphenoxy)methyl)oxirane (10). To a stirring mixture of NaOH (363 mg, 9.09 mmol), K_2CO_3 (2.5 g, 18.28 mmol), guaiacol (1.12 g, 9.09 mmol), and tetra-*n*-butylammonium bromide (295 mg, 0.91 mmol) was added (*R*)-epichlorohydrin (1.26g, 13.61 mmol), and the mixture was placed in the microwave vessel. The reaction vessel was heated at 110 °C for 5 min using microwave irradiation. After cooling, the reaction mixture was diluted with H_2O (15 mL), extracted with EtOAc (60 mL), washed with brine (15 mL), and dried (Na_2SO_4). The organic layer was concentrated and then purified by silica gel column chromatography (10% EtOAc/hexanes) to yield compound **10** (530 mg). ^{1}H NMR ($CDCl_3$) δ 2.73−2.74 (dd, 1H), 2.88−2.90 (dd, 1H), 3.80−3.90 (m, 1H), 3.86 (s, 3H), 4.02−4.06 (dd, 1H), 4.21−4.25 (dd, 1H), 6.89−6.95 (m, 4H). ^{13}C NMR ($CDCl_3$) δ 44.7, 49.9, 55.6, 69.9, 111.7, 114.0, 120.6, 121.7, 147.7, 149.4.

(*S*)-1-Fluoro-3-(2-methoxyphenoxy)propan-2-ol (11). To a stirring solution of compound **10** (50 mg, 0.27 mmol) in toluene (1 mL) was added tetra-*n*-butylammonium fluoride (1.0 M, 1.7 mL), and the mixture was heated to 80 °C for 3 h. The reaction mixture was diluted with H_2O (15 mL) and then extracted with EtOAc (60 mL). The organic layer was washed with brine (15 mL), dried (Na_2SO_4), and concentrated. It was further purified by silica gel column chromatography (5% MeOH/$CHCl_3$) to give compound **11** (23 mg, 41%). ^{1}H NMR ($CDCl_3$) δ 3.86 (s, 3H), 4.06−4.14 (m, 2H), 4.21−4.27 (dd, 2H), 4.48−4.67 (dd, 2H), 6.89−7.01 (m 4H). ^{13}C NMR ($CDCl_3$) δ 55.9, 69.0 (d, J_{C-F} = 20.45 Hz, 1C), 70.6, (d, J_{C-F} = 6.59 Hz, 1C), 83.7 (d, J_{C-F} = 170.04 Hz, 1C). ESI-MS (M + Na^+): calculated, 223.30; found, 223.0. $[\alpha]_D^{23.6}$ +20.51° (*c* 1.95, DCM).

Bioassays for (*R*/*S*)-1 and (*R*)-1. Assay protocol using plasma samples included the following procedure: A 50 μM solution of (*R*/*S*)-3-(2-trifluoromethoxyphenoxy)-1,2-propanediol in water was used as an internal standard (IS). IS response was variable and was not used in quantification. Working standard solutions for either *R*-guaifenesin or *R*-guaifenesin toluyl ester were 20, 50, 200, 500, 2000, 5000, 20 000, 50 000, 100 000 nM in water. All plasma samples in the Eppendorf tubes were capped and vortexed for 2 min followed by centrifugation at 3500 rpm for 5 min. The aqueous layer was frozen in dry ice−methanol bath, and the organic layer was transferred into 16 × 100 mm culture tubes (catalog no. 47729-576). Organic solvent was dried under N_2 stream (10 psi) at room temperature for 30 min. Each sample was then reconstituted in 100 μL of 0.2% TFA in MeOH/water, 20:80, and transferred into 96-well plates for LC−MS/MS analysis.

Assessment of Neurite Outgrowth in Vitro. DRG from adult male Sprague−Dawley rats were dissociated using a previously described method.[20,31,32] Neurons were cultured in defined Hams

dx.doi.org/10.1021/jm400401y | J. Med. Chem. XXXX, XXX, XXX−XXX

F12 medium in the presence of modified Bottensteins N2 supplement without insulin (0.1 mg/mL transferrin, 20 nM progesterone, 100 μM putrescine, 30 nM sodium selenite, 1.0 mg/mL BSA; all additives were from Sigma, St. Louis, MO, U.S.; culture medium was from Life Technologies, Grand Island, NY, U.S.). Quantification of relative neurite outgrowth of adult rat DRG neurons was used as an index to assess drug efficacy compared to control neurons of the same specimen. Total neurite length (the sum of the length of all the neurites produced by an individual neuron) was evaluated and has previously been validated as an in vitro measure of axonal collateral sprouting in vivo.[30] This parameter in the treated culture was examined by confocal microscopy. Captured DIC images of the DRG culture after a 24 h incubation with the test compounds were obtained with a Zeiss LSM 510 confocal microscope. This method of image capture provided quality images with optimal resolution through Nunc optical glass culture well bottoms. Zeiss proprietary LSM file format was batch-converted into TIFF format by use of a file converter plugin from Image J Analysis Software, version 4.0e (NIH). The total axon outgrowth of these neurons was then measured using image analysis software (SigmaScan Pro, Systat Sofware Inc., Point Richmond, CA, U.S.). The total neurite outgrowth was determined by placing a standardized 1.5 cm × 1.5 cm square grid image overlay on the image and counting the total number of intercepts with the grid line. This morphometric approach, based upon a Weibel grid, provided an accurate measure of total neurite length either in relative units (number of crosspoints/cell) or in absolute units (μm/cell).[31,32]

This cell culture procedure has the advantage of being derived from primary adult neurons; however, a drawback is variation in absolute levels of neurite outgrowth observed between each preparation. The level of variability within each experiment can also be high on some occasions because of low neuron yield. To circumvent these limitations, each independent experiment was repeated at least 3 times.

In Vivo Therapeutic Efficacy Studies. All studies were performed in adult female C57 BL/6J mice (Jackson Laboratories) maintained under standard vivarium conditions with free access to food (LabDiet 5001, Purina) and water. Insulin deficient type 1 diabetes was induced by intraperitoneal injection of 90 mg/kg STZ (Sigma Chemicals) in sterile citrate buffer to fasted mice on 2 consecutive days. Diabetes was confirmed 4 days later and at the end of each study by measuring glucose concentration in a blood sample obtained by tail prick using a strip operated reflectance meter (One-Touch Ultra, Lifescan Inc.). Sciatic nerve MNCV was measured at 37 °C in isoflurane-anesthetized mice using electrodes placed at the sciatic notch and Achilles tendon to deliver 5 V for 0.05 ms single square wave stimuli and recording electrodes placed within the interosseus muscles of the ipsilateral paw, exactly as described elsewhere.[33] Guaifenesin or vehicle (water) was delivered by oral gavage 6 days per week from the onset of diabetes. Data are presented as group mean ± SEM with statistical comparisons made by one-way ANOVA with Dunnett's post hoc test.

In Vitro PAMPA Assay. PAMPA (parallel artificial membrane permeability assay) was performed in a 96-well BD Gentest precoated PAMPA plate system (BD Biosciences, Woburn, MA). Prior to use, the precoated PAMPA plate system was warmed to room temperature for 30 min and 325 μL of 25 μM solution for compound (*R*)-**1** or (*S*)-**1** in 5% DMSO in phosphate buffered saline (PBS) was added into wells in the receiver (donor) plate. Then 200 μL of 5% DMSO in PBS was added into wells in the filter (acceptor) plate. The filter plate was placed on the receiver plate by slowly lowering the precoated PAMPA plate until it sits on the receiver plate. The assembly was incubated in a water bath at 25 °C for 5 h. After incubation, buffer samples collected from the acceptor plate and the donor plate, together with calibration standard samples, were prepared in 96-well plates. The plates were then capped, vortexed, and centrifuged at 3000 rpm for 10 min. The supernatant was injected into LC−MS/MS and was analyzed for the compounds using standard protocol.

In Vitro Metabolic Stability Study. Compounds (*R*)-**1** and (*S*)-**1** were investigated for their metabolic stability in mouse and human liver microsomes. Test compounds and the control (propranolol) were incubated at 2 μM with mouse and human liver microsomes in the presence of an excess of NADPH. The incubations ($n = 6$), conducted in 0.5 mL 96-well plates in a shaking water bath maintained at 37 °C, were performed for 0 and 60 min and quenched by the addition of 2 volumes of acetonitrile. After incubation, the plates were then capped, vortexed, and centrifuged at 3000 rpm for 10 min. Then 150 μL of supernatant was transferred into Eppendorf deepwell 96/500 μL plates and diluted with 150 μL of water. The final analytical plates were then capped, vortexed, and centrifuged at 3000 rpm for 10 min. The supernatant was injected into the LC−MS/MS instrument.

■ ASSOCIATED CONTENT

Ⓢ Supporting Information

Purity data for compounds. This material is available free of charge via the Internet at http://pubs.acs.org.

■ AUTHOR INFORMATION

Corresponding Author

*Mailing address: No. 5-356, Toronto Medical Discoveries Tower/MaRS Center, 101 College Street, Toronto, Ontario M5G 1L7, Canada. Phone: (416) 581-7601. E-mail: lkotra@uhnres.utoronto.ca.

Notes

The authors declare no competing financial interest.

■ ACKNOWLEDGMENTS

We acknowledge the support by Juvenile Diabetes Research Foundation (JDRF) Grant No. 14-2006-341 to P.F. and JDRF Grant No. 17-2008-1047 to P.F., L.P.K., and N.A.C. We acknowledge excellent technical support from Drumetix Laboratories (Greensboro, NC, U.S.) for the liver microsomal and PAMPA assays.

■ ABBREVIATIONS USED

DRG, dorsal root ganglia; STZ, streptozotocin; MNCV, motor neuron conduction velocity; NCV, neuron conduction velocity; PAMPA, parallel artificial membrane permeability assay; IS, internal standard; PBS, phosphate buffered saline

■ REFERENCES

(1) *Screening for Type 2 Diabetics. Report of a World Health Organization and International Diabetes Federation Meeting*; World Health Organization: Geneva, Switzerland, 2003.

(2) Fradkin, J. E. Confronting the urgent challenge of diabetes: an overview. *Health Aff. (Millwood)* **2012**, *31*, 12−19.

(3) Fradkin, J. E.; Roberts, B. T.; Rodgers, G. P. What's preventing us from preventing type 2 diabetes? *N. Engl. J. Med.* **2012**, *367*, 1177−1179.

(4) Pop-Busui, R.; Lu, J.; Lopes, N.; Jones, T. L.; BARI 2D Investigators.. Prevalence of diabetic peripheral neuropathy and relation to glycemic control therapies at baseline in the BARI 2D cohort. *J. Peripher. Nerv. Syst.* **2009**, *14*, 1−13.

(5) Tesfaye, S.; Selvarajah, D. The Eurodiab study: What has this taught us about diabetic peripheral neuropathy? *Curr. Diabetes Rep.* **2009**, *9*, 432−434.

(6) Carrington, A. L.; Shaw, J. E.; Van Schie, C. H.; Abbott, C. A.; Vileikyte, L.; Boulton, A. J. Can motor nerve conduction velocity predict foot problems in diabetic subjects over a 6-year outcome period? *Diabetes Care* **2002**, *25*, 2010−2015.

(7) Dyck, P. J.; Carter, R. E.; Litchy, W. J. Modeling nerve conduction criteria for diagnosis of diabetic polyneuropathy. *Muscle Nerve* **2011**, *44*, 340−345.

(8) Bril, V.; Tomioka, S.; Buchanan, R. A.; Perkins, B. A.; mTCNS Study Group.. Reliability and validity of the modified Toronto clinical neuropathy score in diabetic sensorimotor polyneuropathy. *Diabetes Med.* **2009**, *26*, 240−246.

(9) Albers, J. W.; Herman, W. H.; Pop-Busui, R.; Feldman, E. L.; Martin, C. L.; Cleary, P. A.; Waberski, B. H.; Lachin, J. M.; Diabetes Control and Complications Trial/Epidemiology of Diabetes Interventions and Complications Research Group.. Effect of prior intensive insulin treatment during the diabetes control and complications trial (DCCT) on peripheral neuropathy in type 1 diabetes during the epidemiology of diabetes interventions and complications (EDIC) study. *Diabetes Care* **2010**, *33*, 1090−1096.
(10) Fernyhough, P. Axon Regeneration from Adult Sensory Neurons. U.S. Patent 2008/0255062 A1, October 16, 2008; University of Manitoba, Canada.
(11) Hudack, R. A., Jr.; Barta, N. S.; Guo, C.; Deal, J.; Dong, L.; Fay, L. K.; Caprathe, B.; Chatterjee, A.; Vanderpool, D.; Bigge, C.; Showalter, R.; Bender, S.; Augelli-Szafran, C. E.; Lunney, E.; Hou, X. Design, synthesis, and biological activity of novel polycyclic aza-amide FKBP12 ligands. *J. Med. Chem.* **2006**, *49*, 1202−1206.
(12) Wu, X.; Wan, Y.; Mahalingam, A. K.; Murugaiah, A. M.; Plouffe, B.; Botros, M.; Karlén, A.; Hallberg, M.; Gallo-Payet, N.; Alterman, M. Selective angiotensin II AT2 receptor agonists: arylbenzylimidazole structure−activity relationships. *J. Med. Chem.* **2006**, *49*, 7160−7168.
(13) Van Overmeire, I.; Boldin, S. A.; Dumont, F.; Van Calenbergh, S.; Slegers, G.; De Keukeleire, D.; Futerman, A. H.; Herdewijn, P. Effect of aromatic short-chain analogues of ceramide on axonal growth in hippocampal neurons. *J. Med. Chem.* **1999**, *42*, 2697−2705.
(14) de Medina, P.; Paillasse, M. R.; Payré, B.; Silvente-Poirot, S.; Poirot, M. Synthesis of new alkylaminooxysterols with potent cell differentiating activities: identification of leads for the treatment of cancer and neurodegenerative diseases. *J. Med. Chem.* **2009**, *52*, 7765−7777.
(15) Takebayashi, M.; Hayashi, T.; Su, T. P. Nerve growth factor-induced neurite sprouting in PC12 cells involves sigma-1 receptors: implications for antidepressants. *J. Pharmacol. Exp. Ther.* **2002**, *303*, 1227−1237.
(16) Rossi, D.; Pedrali, A.; Urbano, M.; Gaggeri, R.; Serra, M.; Fernández, L.; Fernández, M.; Caballero, J.; Ronsisvalle, S.; Prezzavento, O.; Schepmann, D.; Wuensch, B.; Peviani, M.; Curti, D.; Azzolina, O.; Collina, S. Identification of a potent and selective σ_1 receptor agonist potentiating NGF-induced neurite outgrowth in PC12 cells. *Bioorg. Med. Chem.* **2011**, *19*, 6210−6224.
(17) Namsolleck, P.; Boato, F.; Schwengel, K.; Paulis, L.; Matho, K. S.; Geurts, N.; Thöne-Reineke, C.; Lucht, K.; Seidel, K.; Hallberg, A.; Dahlöf, B.; Unger, T.; Hendrix, S.; Steckelings, U. M. AT2-receptor stimulation enhances axonal plasticity after spinal cord injury by upregulating BDNF expression. *Neurobiol. Dis.* **2013**, *51*, 177−191.
(18) Guimond, M. O.; Wallinder, C.; Alterman, M.; Hallberg, A.; Gallo-Payet, N. Comparative functional properties of two structurally similar selective nonpeptide drug-like ligands for the angiotensin II type-2 (AT(2)) receptor. Effects on neurite outgrowth in NG108-15 cells. *Eur. J. Pharmacol.* **2013**, *699*, 160−171.
(19) Fernyhough, P. Axon Regeneration from Adult Sensory Neurons. U.S. Patent US20080255062 A1, October 16, 2008.
(20) Huang, T. J.; Sayers, N. M.; Verkhratsky, A.; Fernyhough, P. Neurotrophin-3 prevents mitochondrial dysfunction in sensory neurons of streptozotocin-diabetic rats. *Exp. Neurol.* **2005**, *194*, 279−283.
(21) Jolivalt, C. G.; Lee, C. A.; Ramos, K. M.; Calcutt, N. A. Allodynia and hyperalgesia in diabetic rats are mediated by GABA and depletion of spinal potassium-chloride co-transporters. *Pain* **2008**, *140*, 48−57.
(22) Dyck, P. J.; Albers, J. W.; Andersen, H.; Arezzo, J. C.; Biessels, G. J.; Bril, V.; Feldman, E. L.; Litchy, W. J.; O'Brien, P. C.; Russell, J. W. Diabetic polyneuropathies: update on research definition, diagnostic criteria and estimation of severity. *Diabetes Metab. Res. Rev.* **2011**, *27*, 620−628.
(23) Tomlinson, D. R.; Holmes, P. R.; Mayer, J. H. Reversal, by treatment with an aldose reductase inhibitor, of impaired axonal transport and motor nerve conduction velocity in experimental diabetes mellitus. *Neurosci. Lett.* **1982**, *31*, 189−193.
(24) Calcutt, N. A.; Mizisin, A. P.; Kalichman, M. W. Aldose reductase inhibition, Doppler flux and conduction in diabetic rat nerve. *Eur. J. Pharmacol.* **1994**, *251*, 27−33.
(25) Cameron, N. E.; Cotter, M. A.; Dines, K. C.; Maxfield, E. K.; Carey, F.; Mirrlees, D. J. Aldose reductase inhibition, nerve perfusion, oxygenation and function in streptozotocin-diabetic rats: dose-response considerations and independence from a myo-inositol mechanism. *Diabetologia* **1994**, *37*, 651−663.
(26) Greene, D. A.; Arezzo, J. C.; Brown, M. B. Effect of aldose reductase inhibition on nerve conduction and morphometry in diabetic neuropathy. Zenarestat Study Group. *Neurology* **1999**, *53*, 580−591.
(27) Crankshaw, D. P.; Raper, C. Some studies on peripheral actions of mephenesin, methocarbamol and diazepam. *Br. J. Pharmacol.* **1968**, *34*, 579−590.
(28) Wang, G.; Burczynski, F. J.; Hasinoff, B. B.; Zhang, K.; Lu, Q.; Anderson, J. E. Development of a nitric oxide-releasing analogue of the muscle relaxant guaifenesin for skeletal muscle satellite cell myogenesis. *Mol. Pharmaceutics* **2009**, *6*, 895−904.
(29) Beiswenger, K. K.; Calcutt, N. A.; Mizisin, A. P. Dissociation of thermal hypoalgesia and epidermal denervation in streptozotocin-diabetic mice. *Neurosci. Lett.* **2008**, *442*, 267−272.
(30) Smith, D. S.; Skene, J. H. A transcription-dependent switch controls competence of adult neurons for distinct modes of axon growth. *J. Neurosci.* **1997**, *17*, 646−658.
(31) Fernyhough, P.; Willars, G. B.; Lindsay, R. M.; Tomlinson, D. R. Insulin and insulin-like growth factor I enhance regeneration in cultured adult rat sensory neurones. *Brain Res.* **1993**, *607*, 117−124.
(32) Gardiner, N. J.; Fernyhough, P.; Tomlinson, D. R.; Mayer, U.; von der Mark, H.; Streuli, C. H. Alpha7 integrin mediates neurite outgrowth of distinct populations of adult sensory neurons. *Mol. Cell. Neurosci.* **2005**, *28*, 229−240.
(33) Mixcoatl-Zecuatl, T.; Jolivalt, C. G. A spinal mechanism of action for duloxetine in a rat model of painful diabetic neuropathy. *Br. J. Pharmacol.* **2011**, *164*, 159−169.